

1998

Bayesian hierarchical analysis of minefield data

Noel A. Cressie
Iowa State University, ncressie@uow.edu.au

Andrew B. Lawson
University of Abertay Dundee

Follow this and additional works at: <https://ro.uow.edu.au/infopapers>



Part of the [Physical Sciences and Mathematics Commons](#)

Recommended Citation

Cressie, Noel A. and Lawson, Andrew B.: Bayesian hierarchical analysis of minefield data 1998, 930-940.
<https://ro.uow.edu.au/infopapers/2512>

Research Online is the open access institutional repository for the University of Wollongong. For further information contact the UOW Library: research-pubs@uow.edu.au

Bayesian hierarchical analysis of minefield data

Abstract

Based on remote sensing of a potential minefield, point locations are identified, some of which may not be mines. The mines and mine-like objects are to be distinguished based on their point patterns, although it must be emphasized that all we see is the superposition of their locations. In this paper, we construct a hierarchical spatial point-process model that accounts for the different patterns of mines and mine-like objects and uses posterior analysis to distinguish between them. Our Bayesian approach is applied to COBRA image data obtained from the NSW Coastal Systems Station, Dahlgren Division, Panama City, Florida. 2003 Copyright SPIE - The International Society for Optical Engineering.

Keywords

analysis, hierarchical, minefield, data, bayesian

Disciplines

Physical Sciences and Mathematics

Publication Details

Cressie, N. A. & Lawson, A. (1998). Bayesian hierarchical analysis of minefield data. Proceedings of SPIE - The International Society for Optical Engineering, Detection and Remediation Technologies for Mines and Minelike Targets III (pp. 930-940).

Bayesian hierarchical analysis of minefield data

Noel Cressie^a and Andrew B. Lawson^b

^aDepartment of Statistics, Iowa State University, Ames, IA 50011 USA

^bMathematical Sciences Division, School of Informatics, University of Abertay Dundee, Bell St., Dundee DD1 1HG UK

ABSTRACT

Based on remote sensing of a potential minefield, point locations are identified, some of which may not be mines. The mines and mine-like objects are to be distinguished based on their point patterns, although it must be emphasized that all we see is the superposition of their locations. In this paper, we construct a hierarchical spatial point-process model that accounts for the different patterns of mines and mine-like objects and uses posterior analysis to distinguish between them. Our Bayesian approach is applied to COBRA image data obtained from the NSWC Coastal Systems Station, Dahlgren Division, Panama City, Florida.

Keywords and phrases: Cox point process, Markov chain Monte Carlo, Poisson point process, posterior distribution, prior distribution

1. INTRODUCTION

A problem of high priority for the US Navy and the US Marine Corps is the detection of minefields using remote-sensing technology. Typically, not only are mines (MI) present but also mine-like objects (ML) that are often referred to as “clutter”. The problem of detection of a minefield in the presence of clutter can be abstracted to that of detecting a spatial pattern within a set of point locations made up of both MI and ML locations.

Through the use of an unmanned aerial vehicle equipped with a passive multispectral video sensor subsystem, the Advanced Technology Demonstration called the COBRA (Coastal Battlefield Reconnaissance and Analysis) Program detects and locates minefield and obstacles.¹

The video imagery from the airborne subsystem is transmitted to a ground station subsystem, where it is processed. All six spectral bands are used in a hypothesis-testing strategy to make declarations as to the presence of a MI or a ML at various locations throughout the scene.^{1,2} Thus, based on a point pattern of locations, some of which may be mines and some of which may be clutter (metal objects, rocks, false positives), the analyst attempts to detect and locate the minefields.

Several statistical modeling approaches have been taken, based on the expectation that the spatial pattern of mines is different from that of the clutter. An assumption that the minefield is a region of elevated intensity has been made in several papers.^{2,3,4} An alternative methodology^{5,6} assumes approximate collinearity of mines in the presence of random clutter. A very flexible, Bayesian methodology that is adaptable to these and other assumptions about the mine and clutter patterns, has been recently proposed.⁷ In this paper, we shall refine and implement this Bayesian methodology on minefield data from the COBRA Program (made available by the NSWC Coastal Systems Station in Panama City, Florida).

Section 2 presents the Bayesian hierarchical point-process model that will be used to analyze minefield data made up of the superposition of MIs and MLs in a bounded region $A \subset \mathbb{R}^2$. A Markov chain Monte Carlo (MCMC) algorithm used for simulating the posterior distribution of MI locations, number of MIs, and all parameters of the hierarchical model, is described in Section 3. Analysis of the COBRA data is given in Section 4, and discussion of our approach is given in Section 5.

Further author information -

N.C. (correspondence): Email: ncressie@iastate.edu; Telephone: 515-294-3441; Fax: 515-294-4040

A.B.L.: Email: a.lawson@tay.ac.uk

2. BAYESIAN HIERARCHICAL POINT-PROCESS MODEL

The locations of mines (MIs) or mine-like objects (MLs) in a region A are determined from video imagery and a hypothesis-testing strategy.^{1,2} We assume that A is a bounded open subset of \mathbb{R}^2 in which n_a MIs occur at locations

$$\{y_{a,1}, \dots, y_{a,n_a}\},$$

and n_b MLs occur at locations

$$\{y_{b,1}, \dots, y_{b,n_b}\}.$$

However, it is only the superposition of these two point processes that one observes, namely

$$n = n_a + n_b$$

and

$$\{y_1, \dots, y_n\} = \left(\bigcup_{i=1}^{n_a} \{y_{a,i}\} \right) \cup \left(\bigcup_{j=1}^{n_b} \{y_{b,j}\} \right).$$

Our goal is to predict n_a and $\{y_{a,1}, \dots, y_{a,n_a}\}$, the number of MIs and their locations, from observations n and $\{y_1, \dots, y_n\}$. (By implication, this also yields the number and locations of MLs.)

The approach we take is decidedly Bayesian and involves three levels of a hierarchical spatial statistical model. The first level assumes that, conditional on MI intensity function $\mu_a(\cdot)$ and ML intensity function $\mu_b(\cdot)$, MI and ML locations are distributed independently, according to inhomogeneous Poisson point processes (e.g., [8], p. 650). That is, for the MIs, the joint density of n_a and $\{y_{a,i} : i = 1, \dots, n_a\}$ is,

$$f(n_a, \{y_{a,i}\}) = \exp(-\mu_a(A)) \prod_{v \in \{y_{a,i}\}} \mu_a(v),$$

where $\mu_a(A) \equiv \int_A \mu_a(s) ds$. We write,

$$n_a, \{y_{a,i}\} \sim \text{Pois}(\mu_a(\cdot)).$$

Also, for the MLs,

$$n_b, \{y_{b,j}\} \sim \text{Pois}(\mu_b(\cdot)).$$

Assume that the MI and ML Poisson intensity functions can be written as,

$$\begin{aligned} \mu_a(y) &= \lambda_a g(y) \left\{ \sum_{i=1}^{m_a} h_a(y - x_{a,i}) / m_a \right\}; \quad y \in \mathbb{R}^2, \\ \mu_b(y) &= \lambda_b g(y) \left\{ \sum_{j=1}^{m_b} h_b(y - x_{b,j}) / m_b \right\}; \quad y \in \mathbb{R}^2, \end{aligned}$$

respectively. The components λ_a, λ_b are constant background intensities for locations of MIs and MLs that are linked through,

$$\lambda_a = \rho \lambda_b;$$

$g(\cdot)$ is a function meant to capture common heterogeneity of the Poisson intensities, due to things like topography, amount and incidence of sunlight, and vegetation cover; $m_a, \{x_{a,i} : i = 1, \dots, m_a\}$, and $h_a(\cdot)$ are cluster number, cluster centers, and cluster function, respectively, for the MIs; and $m_b, \{x_{b,j} : j = 1, \dots, m_b\}$, and $h_b(\cdot)$ are likewise defined for the MLs. The cluster functions $h_a(\cdot)$ and $h_b(\cdot)$ have the property that they are nonnegative and are normalized to have a unit integral over the plane; Gaussian densities or uniform densities on disks or annuli are often chosen (see Section 4), and we shall denote their parameters by κ_a and κ_b , respectively.

At the second level of the hierarchical spatial statistical model, we assume that cluster number and cluster centers for MIs and MLs are distributed independently, each according to a Strauss point process (e.g., [8], p. 675). That is, the joint density of m_a and $\{x_{a,i} : i = 1, \dots, m_a\}$ is

$$f(m_a, \{x_{a,i}\}) \propto \beta_a^{m_a} \gamma_a^{P(R_a; \{x_{a,i}\})},$$

where β_a is an intensity parameter, $\gamma_a \in [0, 1]$ is an interaction parameter, and

$$P(R_a; \{x_{a,i}\}) \equiv \sum_{i=1}^{m_a} \sum_{k=1}^{m_a} I(\|x_{a,i} - x_{a,k}\| \leq R_a)$$

is the number of unordered pairs of MI cluster centers within distance R_a of each other. We write

$$m_a, \{x_{a,i}\} \sim \text{Strauss}(\beta_a, \gamma_a, R_a) .$$

Also, for the MLs,

$$m_b, \{x_{b,j}\} \sim \text{Strauss}(\beta_b, \gamma_b, R_b) .$$

A fully Bayesian analysis puts a prior distribution on all remaining parameters, namely,

$$(\lambda_a, \kappa_a, \beta_a, \gamma_a, R_a; \rho, \kappa_b, \beta_b, \gamma_b, R_b) \equiv (\theta_a; \theta_b) \sim p .$$

This represents the third and final level of the hierarchy and it is generally where the modeler's subjectivity about the statistical model resides.

The hierarchical spatial statistical model described above is very flexible. For example, suppose it is believed that a minefield is a region B of elevated intensity in the superposed process such as proposed in recent papers.^{2,3,4} One can obtain this model by restricting $m_a = m_b = 1$, $h_a(y) = I(y + x_{a,1} \in B)$, and $h_b(y) = I(y + x_{b,1} \in A)$.

The next stage of the analysis is to write down the joint distribution of all random quantities. Let $[U]$ denote the distribution of the random variable (or random vector) U and $[U|V]$ denote the conditional distribution of U given V . Then the posterior distribution (conditional on observations $n, \{y_i\}$) is,

$$\begin{aligned} & [n_a, \{y_{a,i}\}; m_a, \{x_{a,i}\}, m_b, \{x_{b,j}\}; \theta_a, \theta_b | n, \{y_i\}] \\ & \propto [n_a, \{y_{a,i}\}, n, \{y_i\}; m_a, \{x_{a,i}\}, m_b, \{x_{b,j}\}; \theta_a, \theta_b] , \end{aligned}$$

from which a Gibbs sampler for Bayesian inference can be defined (see Section 3). The Gibbs sampler is a Markov chain Monte Carlo (McMC) algorithm whose realizations are (eventually) those from the Markov chain's stationary distribution, here the posterior distribution. Then, by reporting only the $n_a, \{y_{a,i}\}$ components of the realizations, we obtain samples from the distribution

$$[n_a, \{y_{a,i}\} | n, \{y_i\}] ,$$

from which we can make inference on the MIs (see Section 4).

Before we set out the Gibbs sampler in Section 3, we shall derive a few probabilistic properties of the model. First, since $n, \{y_i\}$ is a superposition of the MI point process and the ML point process, it is clear that $\{y_{a,i}\}$ only has positive probability on subsets of $\{y_i\}$ and that, a.s., $0 \leq n_a \leq n$. It is shown in a previous paper⁷ that, conditional on $\mu_a(\cdot)$ and $\mu_b(\cdot)$,

$$\begin{aligned} & [n_a, \{y_{a,i}\} | n, \{y_i\}; \mu_a(\cdot), \mu_b(\cdot)] \\ & = \prod_{v \in \{y_{a,i}\}} \psi(v) \cdot \prod_{u \in \{y_i\} \setminus \{y_{a,i}\}} (1 - \psi(u)) \cdot I(0 \leq n_a \leq n) \cdot I(\{y_{a,i}\} \subset \{y_i\}) , \end{aligned}$$

where $I(C)$ is 1 if the statement C is true and 0 otherwise;

$$\begin{aligned} \psi(u) & \equiv \mu_a(u) / \{\mu_a(u) + \mu_b(u)\} \\ & = \frac{\rho \left\{ \sum_{i=1}^{m_a} h_a(u - x_{a,i}) / m_a \right\}}{\left\{ \sum_{j=1}^{m_b} h_b(u - x_{b,j}) / m_b \right\}} \\ & = \frac{\rho \left\{ \sum_{i=1}^{m_a} h_a(u - x_{a,i}) / m_a \right\}}{1 + \rho \left\{ \sum_{j=1}^{m_b} h_b(u - x_{b,j}) / m_b \right\}} . \end{aligned}$$

This posterior probability, conditional on $\mu_a(\cdot)$ and $\mu_b(\cdot)$, is available in closed form and shows that the choice, of whether an individual location in the observed point pattern is an MI, is a Bernoulli random variable with success probability given by $\psi(\cdot)$. Of course, $\mu_a(\cdot)$ and $\mu_b(\cdot)$ are in fact random, and hence that variability needs to be integrated out. This cannot be done analytically, giving rise to posterior inference based on simulation methodologies (Section 3).

3. POSTERIOR INFERENCE BASED ON MARKOV CHAIN MONTE CARLO SIMULATION

We shall use a particular Markov chain Monte Carlo (MCMC) simulation method known as the Gibbs sampler (e.g., [9], p.326). The Markov chain is established by sampling successively from the following conditional distributions:

$$\begin{aligned} & [n_a, \{y_{a,i}\} | m_a, \{x_{a,i}\}, m_b, \{x_{b,j}\}; \theta_a, \theta_b; n, \{y_i\}] \\ & [m_a, \{x_{a,i}\}, m_b, \{x_{b,j}\} | \theta_a, \theta_b; n_a, \{y_{a,i}\}, n, \{y_i\}] \\ & [\theta_a, \theta_b | m_a, \{x_{a,i}\}, m_b, \{x_{b,j}\}; n_a, \{y_{a,i}\}, n, \{y_i\}]. \end{aligned}$$

These conditional distributions can each be simplified in different ways. The general approach to the simplification is to inspect the full joint distribution given in Section 2 (and noted there to be proportional to the posterior distribution).

The full joint distribution can be factorized as,

$$\begin{aligned} & [n_a, \{y_{a,i}\}, n, \{y_i\} | m_a, \{x_{a,i}\}, m_b, \{x_{b,j}\}; \theta_a, \theta_b] \cdot [m_a, \{x_{a,i}\}, m_b, \{x_{b,j}\} | \theta_a, \theta_b] \cdot [\theta_a, \theta_b] \\ & = e^{-\mu_a(A)} \prod_{v \in \{y_{a,i}\}} \mu_a(v) \cdot e^{-\mu_b(A)} \prod_{u \in \{y_i\} \setminus \{y_{a,i}\}} \mu_b(u) \cdot I(0 \leq n_a \leq n) \cdot I(\{y_{a,i}\} \subset \{y_i\}) \\ & \cdot \frac{\beta_a^{m_a} \gamma_a^{P(R_a; \{x_{a,i}\})}}{k(\beta_a, \gamma_a, R_a)} \cdot \frac{\beta_b^{m_b} \gamma_b^{P(R_b; \{x_{b,j}\})}}{k(\beta_b, \gamma_b, R_b)} \cdot [\lambda_a, \kappa_a; \rho, \kappa_b] \cdot [\beta_a, \gamma_a, R_a; \beta_b, \gamma_b, R_b]. \end{aligned}$$

Consider a generic joint density $[W, X, Y, \dots]$ that can be factored multiplicatively as a function of arguments w, x, y, \dots . Then $[W|X, Y, \dots]$ is proportional to only those multiplicative factors involving the argument w in the joint factorization. This observation will be used to simplify the conditional distributions of the Gibbs sampler.

After using diagnostic checks that establish convergence of the Markov chain (such as may be found in [9], Section 11.4), we use the last N realizations of the chain to calculate empirical summaries of the posterior distribution. For example, the N realizations of n_a :

$$n_a^{(1)}, \dots, n_a^{(N)},$$

can be used to construct a histogram that is an estimate of $[n_a | n, \{y_i\}]$. Also, for the k -th location y_k in $\{y_i\}$, the N realizations,

$$I\{y_k^{(1)} \text{ is a MI}\}, \dots, I\{y_k^{(N)} \text{ is a MI}\}$$

can be summarized as

$$(1/N) \sum_{l=1}^N I\{y_k^{(l)} \text{ is a MI}\},$$

which is an estimate of the posterior probability, $\Pr(y_k \text{ is a MI} | n, \{y_i\})$.

3.1 Conditional simulation of MI/ML configuration

The first conditional distribution of the Gibbs sampler is easily simplified:

$$\begin{aligned} & [n_a, \{y_{a,i}\} | m_a, \{x_{a,i}\}, m_b, \{x_{b,j}\}; \theta_a, \theta_b; n, \{y_i\}] \\ & \propto \prod_{v \in \{y_{a,i}\}} \mu_a(v) \cdot \prod_{u \in \{y_i\} \setminus \{y_{a,i}\}} \mu_b(u) \cdot I(0 \leq n_a \leq n) \cdot I(\{y_{a,i}\} \subset \{y_i\}), \end{aligned}$$

which we have already seen in Section 2 is (proportional to) the distribution of independent Bernoulli random variables, with the probability of a MI at y_k being $\{\mu_a(y_k)/(\mu_a(y_k) + \mu_b(y_k))\}$. Thus, conditional simulation of $n_a, \{y_{a,i}\}$, given everything else, is straightforward.

3.2 Conditional simulation of MI/ML cluster centers

The second conditional distribution of the Gibbs sampler is not as easily simplified as the first component:

$$[m_a, \{x_{a,i}\}, m_b, \{x_{b,j}\} | \theta_a, \theta_b; n_a, \{y_{a,i}\}, n, \{y_i\}]$$

involves analytically intractable normalizing constants associated with the factors $\gamma_a^{P(R_a; \{x_{a,i}\})}$ and $\gamma_b^{P(R_b; \{x_{b,j}\})}$. Hence, to simulate from the conditional distribution above we use another MCMC method known as the Metropolis-Hastings (MH) sampler¹⁰ with the inclusion of reversible jump steps.^{11,12,13} The MH algorithm has two components, described here for the MI cluster centers: the first simulates a proposal $m'_a, \{x'_{a,i}\}$, possibly to replace the current value $m^o_a, \{x^o_{a,i}\}$; the second either accepts the proposal or retains the current value, each with prespecified probabilities that add to 1. Then, either with the accepted proposal, or the retained current value, the cycle is repeated. A similar simulation is carried out for the ML cluster centers. Consider generic cluster values $m, \{x_i\}$, defined in a region $D = AU\{\text{guard region}\}$ to account for possible cluster centers outside A . Suppose that the current value is $m^o, \{x^o_i\}$ and that the proposal is $m', \{x'_i\}$. The proposal is obtained from the current value by adding (birth) a cluster center, taking away (death) a cluster center, or shifting a cluster center to a different location. Given the current value $m^o, \{x^o_i\}$, define these probability distributions by, respectively,

$$\begin{aligned} b(u) &\propto n^{-1} \sum_{i=1}^n k(u - y_i) ; u \in D , \\ d(v) &= (m^o)^{-1} ; v \in \{x^o_i\} , \\ s(u, v) &= (m^o)^{-1} k(u - v) ; v \in \{x^o_i\}, u \in D , \end{aligned}$$

where, say, $k(x) = \epsilon^{-1} I(0 \leq \|x\| \leq \epsilon)$ and ϵ is a specified bandwidth. Then, given the current value $m^o, \{x^o_i\}$, one obtains the proposal $m', \{x'_i\}$ by simulating from the proposal distribution,

$$\Pr(m', \{x'_i\} | m^o, \{x^o_i\}) \equiv \begin{cases} (1-p)qn^{-1} \sum_{i=1}^n k(u - y_i) ; m' = m^o + 1, \{x'_i\} = \{x^o_i\} \cup u, u \in D , \\ (1-p)(1-q)(m^o)^{-1} ; m' = m^o - 1, \{x'_i\} = \{x^o_i\} \setminus v, v \in \{x^o_i\} , \\ p(m^o)^{-1} k(u - v) ; m' = m^o, \{x'_i\} = (\{x^o_i\} \setminus v) \cup u, v \in \{x^o_i\}, u \in D , \\ 0 ; \text{elsewhere} , \end{cases}$$

where p is a prespecified probability of a shift being proposed and q is a prespecified conditional probability of a birth, given a birth or death is to be proposed.

The MH algorithm specifies that the new value is chosen to be

$$\begin{cases} m', \{x'_i\} , & \text{with probability } \min(1, h) \\ m^o, \{x^o_i\} , & \text{with probability } \max(0, 1 - h) , \end{cases}$$

where h has been derived previously⁷ to be the product of two terms:

$$h = h_1 \cdot h_2 ,$$

such that

$$h_1 = \Pr(m^\circ, \{x_i^\circ\} | m', \{x_i'\}) / \Pr(m', \{x_i'\} | m^\circ, \{x_i^\circ\})$$

$$= \begin{cases} \frac{\binom{1-q}{q} \frac{n}{\sum_{i=1}^{m^\circ+1} k(u-y_i)}}{1} & ; m' = m^\circ + 1, \{x_i'\} = \{x_i^\circ\} \cup u, u \in D, \\ \frac{m^\circ \sum_{i=1}^n k(v-y_i)}{\binom{q}{1-q} \frac{n}{\sum_{i=1}^{m^\circ-1} k(v-y_i)}} & ; m' = m^\circ - 1, \{x_i'\} = \{x_i^\circ\} \setminus v, v \in \{x_i^\circ\}, \\ 1 & ; m' = m^\circ, \{x_i'\} = (\{x_i^\circ\} \setminus v) \cup u, v \in \{x_i^\circ\}, u \in D, \end{cases}$$

and

$$h_2 = \beta^{m'} \gamma^{P(R; \{x_i'\})} / \beta^{m^\circ} \gamma^{P(R; \{x_i^\circ\})}$$

$$= \begin{cases} \beta \gamma^{\sum_{i=1}^{m^\circ} I(|u-x_i^\circ| \leq R)} & ; m' = m^\circ + 1, \{x_i'\} = \{x_i^\circ\} \cup u, u \in D, \\ \beta^{-1} \gamma^{-\sum_{x_i^\circ \neq v} I(|v-x_i^\circ| \leq R)} & ; m' = m^\circ - 1, \{x_i'\} = \{x_i^\circ\} \setminus v, v \in \{x_i^\circ\}, \\ \gamma^{\sum_{i=1}^{m^\circ} I(|u-x_i^\circ| \leq R) - \sum_{x_i^\circ \neq v} I(|v-x_i^\circ| \leq R)} & ; m' = m^\circ, \{x_i'\} = (\{x_i^\circ\} \setminus v) \cup u, v \in \{x_i^\circ\}, u \in D. \end{cases}$$

To generate MI cluster centers, the MH algorithm is used with all variables above subscripted with 'a'. Similarly, ML cluster centers are generated in exactly the same way, now with all variables subscripted with 'b'. Finally, the two cluster-center processes are assumed independent and hence can be generated separately.

3.3 Conditional simulation of "nuisance" parameters

From the point of view of predicting n_a and $\{y_{a,i}\}$, the parameters in θ_a and θ_b are nuisance parameters. They are featured in the third component of the Gibbs sampler:

$$[\theta_a, \theta_b | m_a, \{x_{a,i}\}, m_b, \{x_{b,j}\}; n_a, \{y_{a,i}\}, n, \{y_i\}].$$

Because θ_a includes parameters from both the conditional Poisson process and the Strauss process, there are a number of factors in the joint distribution that include θ_a and θ_b . Therefore, the MH algorithm we use to generate the third component of the Gibbs sampler is not as simple as the previous one. However, in specific applications it can simplify and this is indeed the case when we analyze the COBRA data in the next section.

4. STATISTICAL INFERENCE FOR MI/ML DATA FROM THE COBRA PROGRAM

A brief description of the COBRA Program, one of whose goals is the detection and location of minefields in littoral areas, is given in Section 1. The Bayesian hierarchical analysis described in Sections 2 and 3 was applied to data obtained from the NSWC Coastal Systems Station, Dahlgren Division, Panama City, Florida. Figure 1 shows detected locations of MIs and MLs in a grassy region that has been standardized to the unit square. Although in practice it is not known which of the locations are MIs and which are MLs, the truth is known in this case and the MIs and MLs are distinguished in Figure 1. Of course, in carrying out the analysis, this external knowledge was not used.

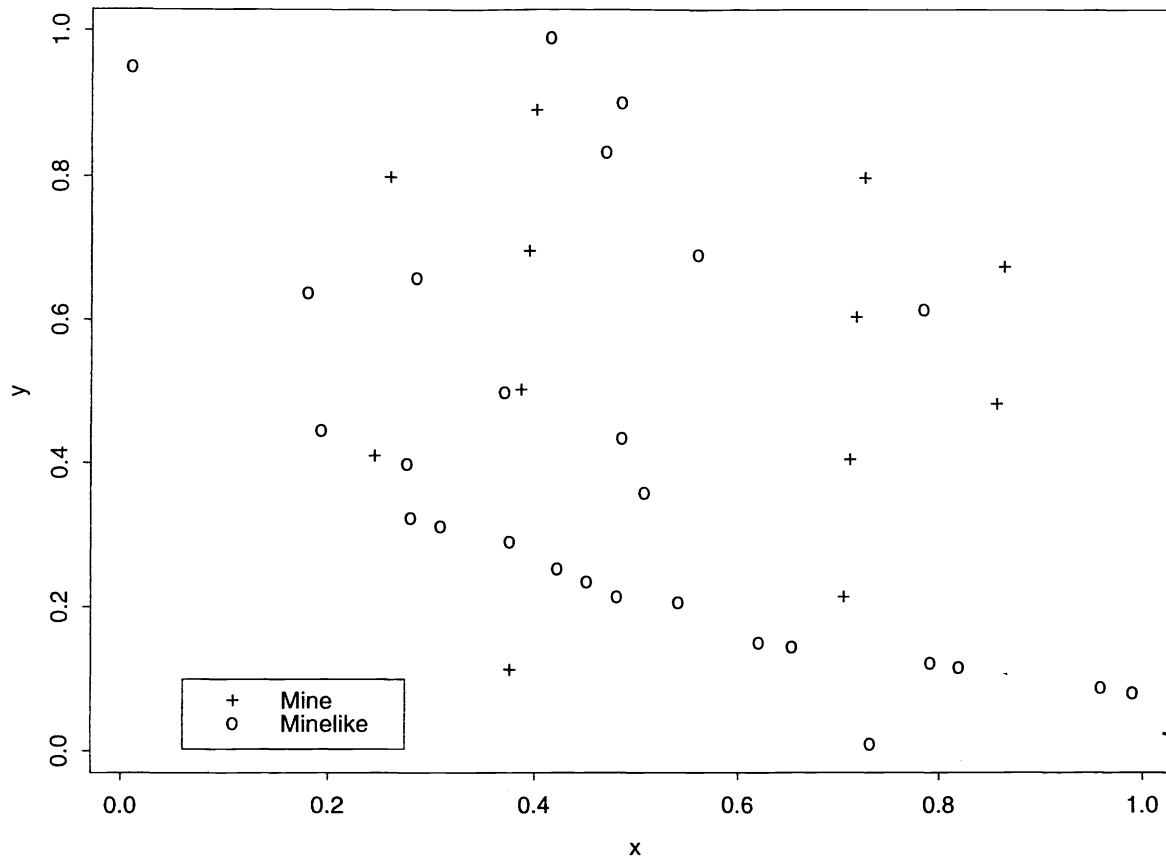


Figure 1: COBRA data showing locations of MIs (pluses) and MLs (disks) in the unit square. Only the superposition of number and location of objects was used in the analysis.

In order to carry out the analysis, some decisions were made about parameters in the hierarchical model defined in Section 2 and about the construction of the Markov chain (from which the Gibbs sampler was implemented) described in Section 3. Recall the notation established in Section 2. We set the heterogeneity component $g(\cdot) \equiv 1$. For the cluster process of MIs, we set

$$h_a(u) \equiv (\pi(.01)^2)^{-1} I(0 \leq \|u\| \leq .01),$$

which is the uniform density on a disk of very small radius ($\kappa_a = .01$), reflecting our belief that MIs are not dispersed at great distances. This, along with the choice of $\gamma_a = .0001$ and $R_a = 0.25$, puts higher prior probability on MIs that are fairly regular and may appear as singles or tightly bound clusters. For the cluster process of MLs, we set

$$h_b(u) = (\pi(.15)^2)^{-1} I(0 \leq \|u\| \leq .15),$$

which allows clusters of considerably larger radius ($\kappa_b = .15$). By setting $\beta_b = 12$, $\gamma_b = 0.5$, and $R_b = 0.25$, we are thinking of cluster centers that are "halfway" between regular and Poisson, and about two MLs per cluster center.

So, this leaves us to specify the prior distributions of just λ_a , λ_b (equivalently, ρ), and β_a . We chose:

$$[\lambda_a] \propto \exp(-.01/\lambda_a),$$

$$[\lambda_b] \propto \exp(-.01/\lambda_b),$$

which are improper priors that penalize small values of λ_a or λ_b . An adaptive method of sampling β_a was chosen and this is described in the next paragraph.

Recall the notation established in Section 3.2. We chose to have no shifting ($p = 0$) and equal probability of birth or death ($q = 1/2$). The kernel $k(\cdot)$ used the bandwidths of $\epsilon_a = .01$ and $\epsilon_b = .15$, reflecting the belief that MI cluster centers are closer to observed locations than ML cluster centers. Also, a guard area was not used so that $D = A$. Finally, an adaptive method of sampling β_a was chosen, by setting it equal to $m_a/|A|$ (which is here just m_a).

Figure 2 shows a three-dimensional scatter plot of

$$Pr\{y_k \text{ is a MI} \mid n, \{y_i\}\} \text{ versus } y_k; \quad k = 1, \dots, n,$$

where the posterior probability is in fact estimated from the last N simulations (here $N = 500$) via,

$$(1/N) \sum_{\ell=1}^N I\{y_k^{(\ell)} \text{ is a MI}\}.$$

Superimposed on Figure 2 is the true identity of each point of the point pattern; MIs should have higher posterior probabilities than MLs, and this is largely the case. Notice that there are quite a few false positives (about half the MLs have noticeable posterior probabilities) but only a small number of false negatives, which is the way we would hope it to be. Given the difficulty of the problem, the Bayesian hierarchical analysis is doing quite a good job of finding the MIs in the presence of clutter.

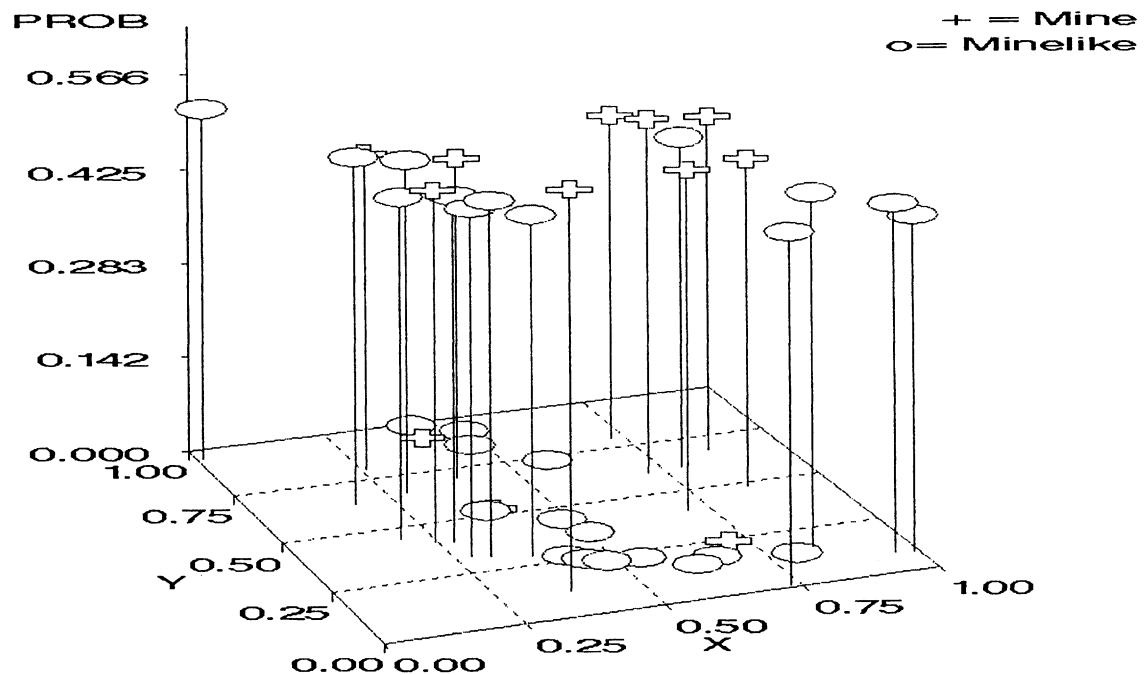


Figure 2: Three-dimensional scatterplot of (estimated) posterior probability that a given location is an MI. The MIs (pluses) and MLs (disks) are the true designation obtained from Figure 1.

Figure 3 shows the posterior distribution,

$$[n_a | n, \{y_i\}] ,$$

which is in fact estimated from the histogram of,

$$n_a^{(1)}, \dots, n_a^{(\ell)}, \dots, n_a^{(N)} .$$

We know that the true value of n_a is 12; from Figure 3, we see that the posterior distribution of n_a is roughly symmetric about its modal value of 11. Again, the Bayesian hierarchical analysis is performing quite well.

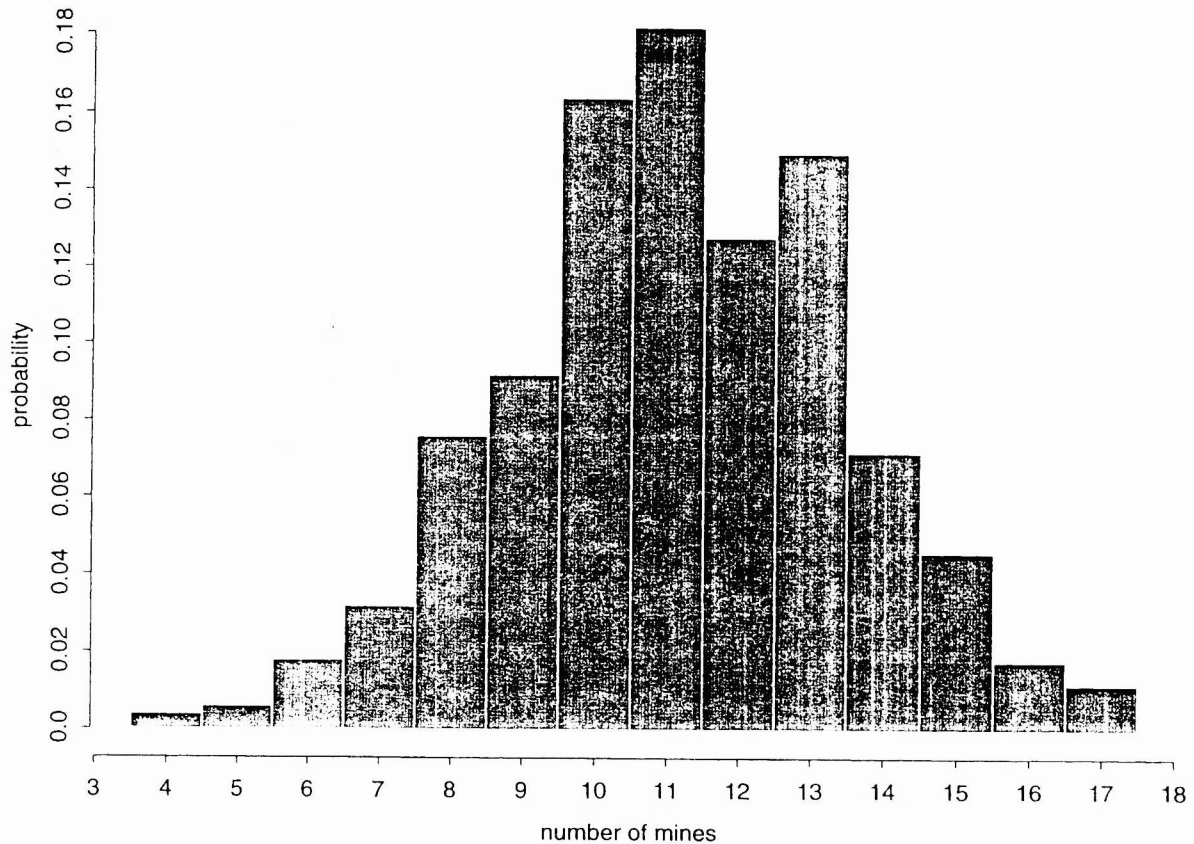


Figure 3: (Estimated) posterior distribution of n_a .

5. DISCUSSION

The Bayesian hierarchical analysis has met with some success in analyzing the COBRA data shown in Figure 1. The output from the Markov chain Monte Carlo algorithm is extremely rich. Posterior distributions of any of the variables, $m_a, \{x_{a,i}\}, m_b, \{x_{b,j}\}, \theta_a, \theta_b$, as well as $n_a, \{y_{a,i}\}$, can be obtained (through empirical estimates).

The strength of our approach is that it is extremely flexible. If intelligence reports indicate that MIs have been laid in a completely different manner, the parameters θ_a can be adjusted accordingly. The less information one has about how MIs and MLs are generated, the more difficulty one has in discriminating between MIs and MLs.

One final comment is that because the original data are in fact pixellated video images, it should be possible to add a level to the hierarchical model that incorporates the images directly. Suppose that there are $P \times Q$ pixels,

$$\{A(p, q) : p = 1, \dots, P; q = 1, \dots, Q\} ,$$

with pixel intensities

$$\{Z(p, q) : p = 1, \dots, P; q = 1, \dots, Q\} .$$

Now, if a MI is at location $y_{a,i}$, we assume that the associated image intensity is given by a point-spread function,

$$Z_{a,i}(u) = (2\pi\sigma_a^2)^{-1/2} \exp\{-(u - y_{a,i})^2/2\sigma_a^2\} .$$

Likewise, for a ML, $Z_{b,j}(u)$ can be defined. Then the total intensity due to MIs is,

$$Z_a(u) = \sum_{i=1}^{n_a} Z_{a,i}(u) ,$$

and the total intensity due to MLs is,

$$Z_b(u) = \sum_{j=1}^{n_b} Z_{b,j}(u) .$$

Thus, conditional on $n_a, \{y_{a,i}\}$ and $n_b, \{y_{b,j}\}$, the pixel intensities can be written as,

$$Z(p, q) = \int_{A(p,q)} \{Z_a(u) + Z_b(u)\} du .$$

The goal is still to predict $n_a, \{y_{a,i}\}$, but the data are now the pixel intensities $\{Z(p, q)\}$.

ACKNOWLEDGMENT

The minefield data was obtained from the NSWC Coastal Systems Station, Dahlgren Division, Panama City, FL. This research was supported by the Office of Naval Research under grant no. N00014-93-1-0001. The authors would like to thank Robert Muise, Cary Priebe, and Jun Zhu for their help in converting the COBRA data files into the point pattern given in Figure 1.

REFERENCES

1. N.H. Witherspoon, J.H. Holloway, K.S. Davis, R.W. Miller, and A.C. Dubey, "The coastal battlefield reconnaissance and analysis (COBRA) program for minefield detection," in *Detection Technologies for Mines and Minelike Targets*, eds. A.C. Dubey, I. Cindrich, J.M. Ralston, and K. Rigano. SPIE Proceedings, Vol. **2496**, Bellingham, WA, pp. 500-508, 1995.
3. S. Byers and A.E. Raffery, "Nearest neighbor clutter removal for estimating features in spatial point processes," Technical Report No. 305, Department of Statistics, University of Washington, Seattle, WA, 1996.
4. C.E. Priebe, T.E. Olson, and D.M. Healy, "Exploiting stochastic partitions for minefield detection," in *Detection and Remediation Technologies for Mines and Minelike Targets II*, eds. A.C. Dubey and R.L. Barnard. SPIE Proceedings, Vol. **3079**, Bellingham, WA, pp. 508-518, 1997.
5. D.E. Lake, B. Sadler, and S. Casey, "Detecting regularity in minefields using collinearity and a modified Euclidean algorithm," in *Detection and Remediation Technologies for Mines and Minelike Targets II*, eds. A.C. Dubey and R.L. Barnard. SPIE Proceedings, Vol. **3079**, Bellingham, WA, pp. 500-507, 1997.
6. R.R. Muise and C.E. Smith, "A linear density algorithm for patterned minefield detection," in *Detection Technologies for Mines and Minelike Targets*, eds. A.C. Dubey, I. Cindrich, J.M. Ralston, and K. Rigano. SPIE Proceedings, Vol. **2496**, Bellingham, WA, pp. 583-593, 1995.

7. N. Cressie and A.B. Lawson, "Models and inference for clustering of locations of mines and mine-like objects," in *Detection and Remediation Technologies for Mines and Minelike Targets II*, eds. A.C. Dubey and R.L. Barnard. SPIE Proceedings, Vol. **3079**, Bellingham, WA, pp. 519–530, 1997.
8. N. Cressie, *Statistics for Spatial Data, revised edition*, Wiley, New York, NY, 1993.
9. A. Gelman, J.B. Carlin, H.S. Stern, and D.B. Rubin, *Bayesian Data Analysis*, Chapman and Hall, London, U.K., 1995.
10. W.K. Hastings, "Monte Carlo sampling methods using Markov chains and their applications," *Biometrika* **57**, pp. 97–109, 1970.
11. C. Geyer and J. Moller, "Simulation procedures and likelihood inference for spatial point processes," *Scandinavian Journal of Statistics* **21**, pp. 359–373, 1994.
12. P.J. Green, "Reversible jump MCMC computation and Bayesian model determination," *Biometrika* **82**, pp. 711–732, 1995.
13. A.B. Lawson, "Markov chain Monte Carlo methods for spatial cluster processes," *Computer Science and Statistics* **27**, pp. 314–319, 1996.